COMPUTER METHODS IN APPLIED MECHANICS AND ENGINEERING 12 (1977) 353–364

THE VIRTUAL CRACK EXTENSION METHOD FOR NONLINEAR MATERIAL BEHAVIOR

D.M. PARKS

Department of Engineering and Applied Science Yale University, New Haven, Connecticut 06520

Received 21 February 1977

The linear elastic, stiffness-derivative, finite element technique of Parks [1] is generalized to determine the ductile fracture parameter J from elastic-plastic finite element solutions. The method, based on energy comparison of two slightly different crack lengths, requires only one elastic-plastic finite element solution, and the altered crack configuration is obtained by changing nodal point positions. The technique is applied to finite element solutions for a deeply cracked, plane-strain bend specimen – a configuration for which J can be otherwise obtained – and the results are encouraging. The extension of the method to obtain arc-length-weighted J values in three-dimensional crack configurations is also proposed.

Introduction

The J integral [2] has been proposed as a ductile fracture parameter by Begley and Landes [3]-[4] and independently by Broberg [5]. Subsequent work has shown that for most materials ductile fracture is not abruptly initiated from a pre-existing flaw, but rather that some stable crack extension under rising load precedes final fracture. Experimentally determined values of J have been successfully correlated with the amount of slow-stable crack growth, necessarily for small amounts of crack extension [6].

The experimental evaluation of J was first made in the energy comparison manner indicated by Rice [7], identifying $J\,\delta l$ as the area between the load-per-unit-thickness/load-point-displacement curves of two planar specimens with cracks differing slightly in length by an amount δl. Subsequent work [8] based upon dimensional analysis related the value of J to certain areas associated with the load/load-point-displacement curve obtained from a single deeply cracked specimen for a number of specimen configurations.

The progress of numerically determining J has thus far been directed mainly toward elastic-plastic finite element solutions by using the fields thus obtained for numerical evaluation of the line integral which defines J in planar configurations [9]. However, this approach is not suited to axisymmetric or three-dimensional crack configurations. Of course, two elastic-plastic finite element solutions with slightly different crack configurations could be performed, and the difference in the resulting load/load-point-displacement curves could be used to obtain J, but computer costs would be prohibitive, especially in three-dimensional crack configurations, where a determination of the variation of J along the crack front would require several three-dimensional elastic-plastic analyses – a hopelessly expensive proposition.

A new finite element method for elastic-plastic evaluation of J is presented, requiring only a single elastic-plastic solution. The procedure is directly applicable to planar and axisymmetric configurations and can be extended straightforwardly to obtain arc-length-weighted average J values along three-dimensional crack fronts. The energy comparison with the slightly altered crack configuration is accomplished by perturbing nodal point positions and processing the data obtained from the solution of the initial configuration.

1. Formulation

Suppose that an elastic-plastic, finite element analysis of a two-dimensional planar crack configuration of unit thickness has been performed, using deformation plasticity theory as the constitutive relation. At any point in the loading, the finite element evaluation of the potential energy can be obtained, given by

$$\begin{aligned} P &= \sum_{elements} \int_{V_i} W \mathrm{d}V_i - [\hat{\boldsymbol{T}}(\overline{\boldsymbol{X}})]^{\mathrm{t}} \overline{\boldsymbol{U}} \\ &= \sum_{elements} \hat{W}_i(\overline{\boldsymbol{X}}, \overline{\boldsymbol{U}}) - [\hat{\boldsymbol{T}}(\overline{\boldsymbol{X}})]^{\mathrm{t}} \overline{\boldsymbol{U}}, \end{aligned} \tag{1}$$

where V_i is the volume of the ith element of the mesh, $W = W(\epsilon_{ij})$ is the strain energy density (a function of total strain alone), $\overline{\boldsymbol{X}}$ and $\overline{\boldsymbol{U}}$ are the vectors of nodal point coordinates and displacements,

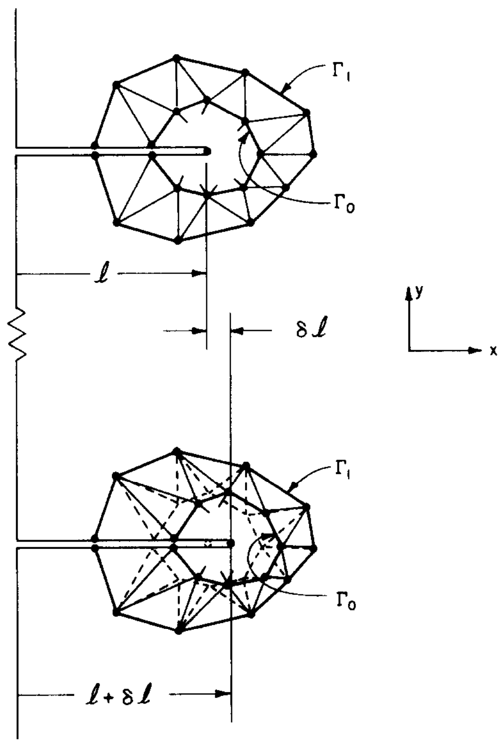

Fig. 1. Schematic illustration of accomodation of virtual crack extension in two-dimensional grid by translating by the amount δl all nodes on and within contour Γ_0.

respectively, $\hat{T}$ is the vector of nodal forces (obtained from consistent distribution of the prescribed tractions and/or body forces) $\hat{W}_i$ is the integral of strain energy over the ith element, and the arguments indicate that the $\hat{W}_i$ depend on the nodal coordinates and displacements. Similarly indicated, the nodal force vector depends on nodal coordinates through the shape functions.

Now consider the virtual crack extension indicated in fig. 1, obtained by incrementing by an amount δl the x-coordinates of all nodes on and within an interior contour Γ_0 which surrounds the crack tip. If higher order elements are used, midside nodes on element boundaries connecting the contours Γ_0 and Γ_1 are advanced by appropriately reduced amounts so as to maintain proper element geometry in the advanced configuration. The variation in the potential energy which this virtual crack advance occasions is

$$\delta P = \sum_{elements} [(\partial \hat{W}_i/\partial \overline{X})^t \delta \overline{X} + (\partial \hat{W}_i/\partial \overline{U})^t \delta \overline{U}] - \hat{T}^t \delta \overline{U} - \overline{U}^t (\partial \hat{T}/\partial \overline{X}) \delta \overline{X}$$

$$= \left[\sum_{elements} (\partial \hat{W}_i/\partial \overline{U})^t - \hat{T}^t \right] \delta \overline{U} + \left[\sum_{elements} (\partial \hat{W}_i/\partial \overline{X})^t - \overline{U}^t (\partial \hat{T}/\partial \overline{X}) \right] \delta \overline{X}. \tag{2}$$

But the coefficient of $\delta \overline{U}$ has presumably been made zero, or arbitrarily small, in the finite element solution, so that the first term in the second line of eq. (2) vanishes. In addition, if the prescribed loading was by other than body forces or crack-face traction, then the variation in the nodal force vector is also zero. Of course, in the general case, this term must be retained, but since it is not essential to the analysis presented here, it will be dropped for convenience. For a fuller treatment see the discussion in [1].

Rice [7] has shown that for planar configurations and deformation theory plasticity the decrease in potential energy with respect to crack length equals the path-independent line integral J; thus, in the finite element discretization,

$$-\delta P = -(\partial P/\partial l)\delta l = +J\delta l = -\sum_{elements} (\partial \hat{W}_i/\partial \overline{X})^t \delta \overline{X}. \tag{3}$$

It should be noted that eq. (3) is a generalization of the energy comparison which Parks [1] and Hellen [10] used to determine stress intensity factors for linear elastic constitutive behavior. In the linear elastic case, $\hat{W}_i$ has the special quadratic form

$$\hat{W}_i = \tfrac{1}{2} \overline{U}^t k_i(\overline{X}) \overline{U}, \tag{4a}$$

and

$$(\partial \hat{W}_i/\partial \overline{X})^t \delta \overline{X} = \tfrac{1}{2} \overline{U}^t \delta k_i \overline{U}, \tag{4b}$$

where the (p,q)-element of δk_i is $\Sigma_r [\partial (k_i)_{pq}/\partial \overline{X}_r] \delta \overline{X}_r$. The name "stiffness-derivative method" is derived from relations (4). Indeed, the method developed here so closely parallels that in [1] that the reader is referred there for additional information.

In finite element solutions of other than two-dimensional planar configurations of unit thickness the same formal steps can be taken in changing nodal positions to obtain virtual crack extensions along an arbitrary crack front, and the potential energy change is

$$-\delta P = \int_{\substack{crack\\front}} J(s)\delta l(s)\mathrm{d}s = -\sum_{elements} (\partial \hat{W}_i/\partial \overline{X})^t \delta X. \tag{5}$$

Thus, by separately advancing individual nodes along a three-dimensional crack front in the plane of the crack, a weighted average of the local J value within the crack front interval enclosing the advanced node(s) can be obtained.

It should be noted that three-dimensional applications of the method need not be restricted to perturbing only nodal coordinates on the crack front, although this choice would be most convenient since the summation indicated in eq. (5) then extends over only the crack front elements joined to the moved node. However, analogous to the two-dimensional axisymmetric application in [1], in three-dimensional configurations the crack front node and certain adjacent nodes not on the crack front may be perturbed in a given virtual crack extension. In such cases the summation indicated in eq. (5) will extend over not only the elements along the crack front but certain adjacent elements as well, and the net effect is that a larger portion of the calculated arc-length-weighted J values will be obtained from regions removed from the immediate crack tip vicinity. This may be desirable, for the author has found that the node-moving procedure generally exhibits greater accuracy at greater distances from the crack tip.

A simplified schematic representation of this aspect of the procedure is illustrated in fig. 2. The four 8-node isoparametric bricks are meant to rest atop a straight segment of crack front adjoining the two middle nodes on the bottom layer. If only the near middle node on the crack front were advanced by δl_0, causing a linear crack front variation $\delta l(s)$, then the sum in eq. (5) need extend only over the bottom two elements. However, if, as indicated in fig. 2, both the crack front node and the node directly above it are advanced – leading to the same $\delta l(s)$ – the sum must then include all four elements.

In the numerical work presented here, all elements used were of the rectangular isoparametric family. The changes in these elements' strain energies were calculated by differencing in the follow-

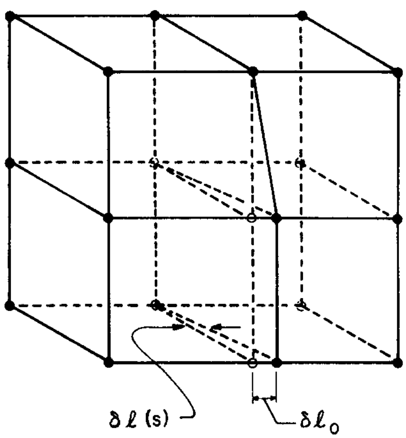

Fig. 2. Schematic illustration of virtual crack extension $\delta l(s)$ in a three-dimensional problem. By advancing both the near node on the crack front and the node directly above it by the same amount δl_0, the strain energies of all four elements are altered and must be included in the summation of eq. (5).

ing manner, due to Hibbitt [11]. Let V_0 be the fixed region in the mapped space where integration over element volumes V_i is performed, and let $|dV_i/dV_0|$ be the absolute value of the Jacobian determinant of the mapping from V_i to V_0. Then

$$\hat{W}_i = \int_{V_0} dV_0 \{W|dV_i/dV_0|\}, \tag{6}$$

so that

$$(1/\delta l)(\partial W_i/\partial \overline{X})^t \delta \overline{X} = \int_{V_0} \{(\partial W/\partial l)|dV_i/dV_0| + W\partial|dV_i/dV_0|/\partial l\}. \tag{7}$$

Since W is a function of strain alone,

$$\partial W/\partial l = (\partial W/\partial \epsilon_{mn})(\partial \epsilon_{mn}/\partial l) = \sigma_{mn}(\partial \epsilon_{mn}/\partial l),$$

and, on substituting into eq. (7),

$$\partial \hat{W}_i/\partial l = \int_{V_0} dV_0 \{|dV_i/dV_0|\sigma_{mn}(\partial \epsilon_{mn}/\partial l) + W\partial|dV_i/dV_0|/\partial l\}. \tag{8}$$

The derivatives indicated in eq. (8) may be approximated by forward differencing. Letting $f(\overline{X}, \overline{U}; \boldsymbol{x}_0)$ stand for any function at the point $\boldsymbol{x}_0$ in V_0,

$$\partial f/\partial l \approx (1/\delta l)[f(\overline{X} + \delta\overline{X}, \overline{U}; \boldsymbol{x}_0) - f(\overline{X}, \overline{U}; \boldsymbol{x}_0)].$$

This derivation can also be applied to incremental plasticity formulations if a W dependent on loading history is defined as

$$W \equiv \int_0^{\epsilon_{mn}} \sigma_{ij} d\epsilon_{ij},$$

where the integration path follows the actual loading trajectory in strain space. Of course, for such incremental plasticity formulations the J integral need not be precisely path-independent over all contours, so the potential energy differences associated with different interior contours of crack advance need not give identical J values, even in the continuum.

Before proceding to numerical details of examples utilizing the method, it is worthwhile to consider some aspects of deformation theory plasticity as applied to finite element analysis of cracks. First, because it is clear on physical grounds that deformation theory plasticity (which is in fact nonlinear elasticity) cannot have general applicability to elastic-plastic analysis, there is a common belief that it can be successfully applied only to cases of proportional plastic stressing, in which case the results would coincide with an incremental theory. But Budiansky [12] showed that deformation theory could be successfully applied to moderately nonradial stress trajectories, provided the actual incremental constitutive relations lead to plastic strains independent of stress trajectory for a limited range of trajectories including (but not restricted to) radial loading. Among the constitutive laws which lead to a limited path independence of plastic strain are the slip theory of plasticity

[13] and the theory of Sanders [14]. In addition, the best available models of polycrystalline deformation [15], [16] lead to plastic strains approximately independent of stress trajectory for moderately nonradial stress histories. A recent discussion of these and other aspects of deformation theory as a model for plastic vertex-forming materials is contained in Stören and Rice [17]. Secondly, in plastic-plastic situations for which J is an appropriate parameter to characterize the environment of a stationary crack tip the loading must be applied by a monotonically increasing loading parameter. Since significant stable crack advance under rising load and its accompanying pronouncedly nonradial load/unload stress trajectories are not allowed, the resultant stress trajectories of all material points generally correspond to moderately nonradial continued plastic loading, although exceptional counterexamples perhaps can be constructed.

For these reasons, then, the use of deformation theory plasticity in the finite element formulation should not cause significant problems within the restricted usage proposed. In addition, tests were placed in the finite element program used to generate the solutions so as to detect unloading or sharply turning stress trajectories should they occur. None were detected. Finally, deformation theory obtains J values which are rigorously path-independent in the continuum, so that application of the node-moving procedure on different contours gives some insight into the accuracy obtainable with the method both near and removed from the crack tip. Results generated using both deformation and incremental theory formulations are presented here.

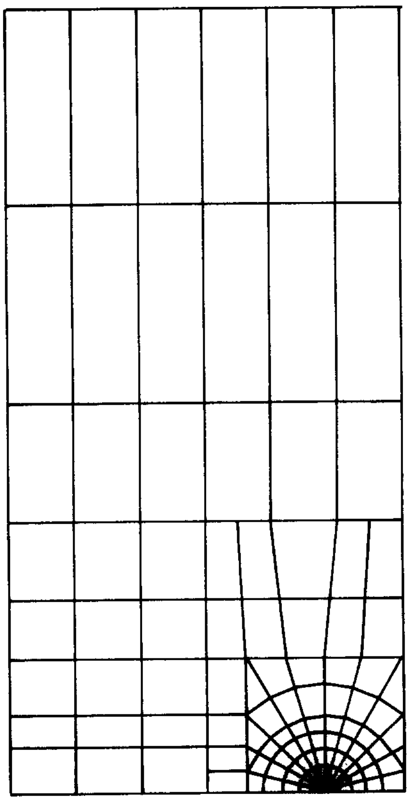

Fig. 3. Mesh of first-order isoparametric elements used to obtain deformation theory solutions of perfectly plastic and power-law hardening behavior.

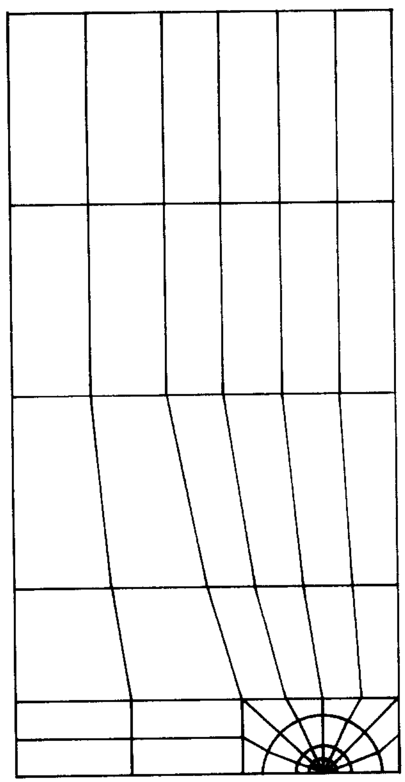

Fig. 4. Mesh of second-order isoparametric elements used to obtain incremental theory perfectly plastic solution.

2. Numerical results

The procedure outlined in the previous section was used to process finite element solutions of a deeply cracked, plane-strain bend specimen. Two different finite element meshes of the specimen (which had a crack depth-to-width ratio of 0.8) were used. The first mesh, shown in fig. 3, consisted of 135 4-node isoparametric elements and 165 nodal points. Surrounding the crack tip were 6 rings of 12 trapezoidal elements focussed to the crack tip. The nodal rings were radially spaced at 0, 0.10, 0.35, 0.55, 0.75 and 1 times the uncracked ligament. The elements of the inner ring were singular, possessing 2 independent nodal points located at the crack tip. The resulting nonuniqueness of crack tip displacement leads, in these elements, to singularities of order r^{-1} in both deviatoric and dilatational strains. Although it was realized that this formulation did not closely adhere to the precise near-tip fields obtained by Rice [1], Hutchinson [18] and Rice and Rosengren [19], nor to the fields modeled with finite elements by Rice and Tracey [20] and Tracey [21], no attempt was made to constrain the crack tip nodal displacements at any point in the loading. Also used was the mesh of fig. 4, which consisted of 54 8-node isoparametric elements and 182 nodes. Wrapped around the crack tip were 4 rings of 8 elements. The radial spacing of the interelement boundaries were 0, 0.05, 0.15, 0.50 and 1 times the remaining uncracked ligament, and all non-corner nodes were located at element midsides. However, all nodes at the cracked tip were constrained to have the same displacement. In a sense, the elements on the inner ring became complete quadratic 6 node triangular elements.

For the 4-node mesh, the problem was solved using two different constitutive laws – perfect plasticity and power-law hardening with a strain-hardening exponent of $N = 0.1$. The plasticity was

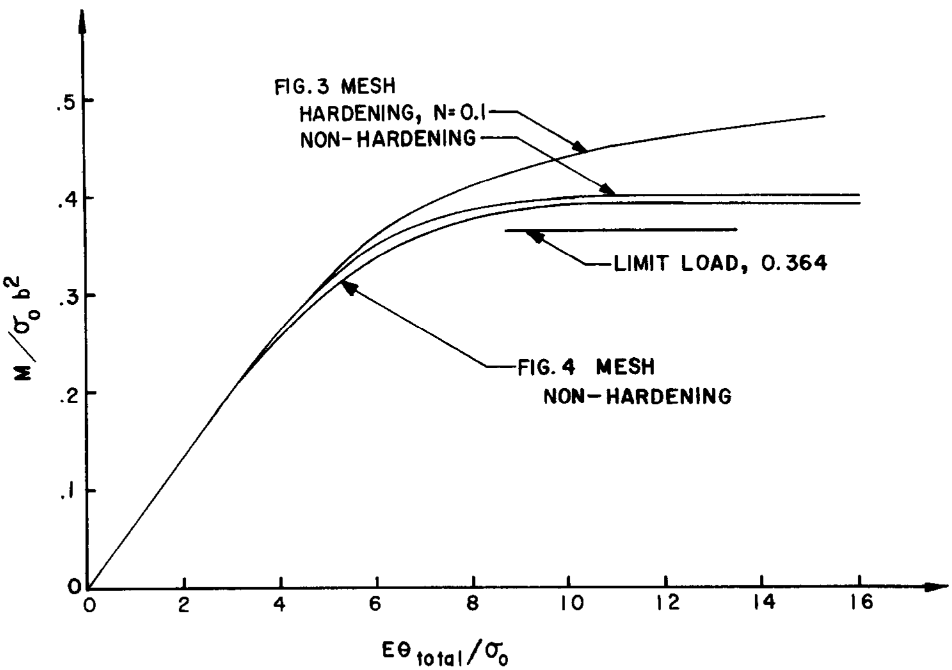

Fig. 5. Overall moment/rotation curves.

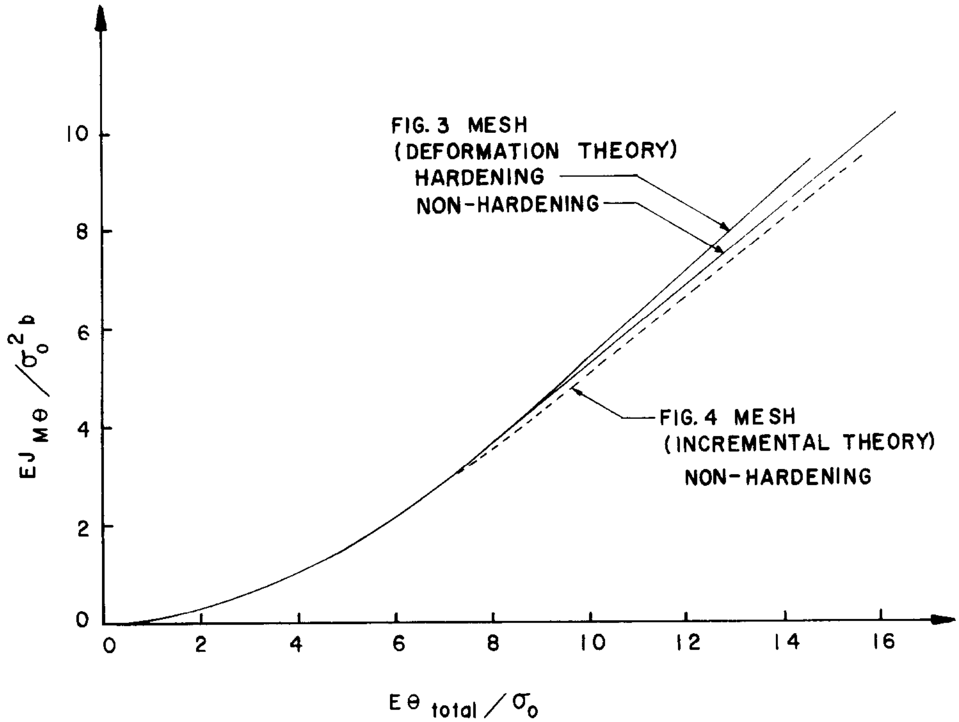

Fig. 6. J values inferred from moment/rotation curves using eq. (11).

modeled using deformation theory. For the mesh of 8-node elements, ideal incremental theory plasticity was used. In all cases a Mises yield criterion was used.

Because it was anticipated that loading would be carried to large plastic deformations, the lower order dilatation elements of Nagtegaal et al. [22], which are suitable for the analysis of incompressible or nearly incompressible behavior encountered in the fully plastic range, were used in the 4-node element mesh. The lower order dilatation procedure was not applied to the 8-node elements, however, but no evidence of artificial constraints of the type which Nagtegaal et al. considered was found in these problems.

The finite element moment/rotation curves are shown in fig. 5. As can be seen, the deformation-theory, perfectly plastic solution using the 4-node elements exceeds the limit load obtained by Green and Hundy [23] by roughly 11 percent, but the curve is very flat in the fully plastic regime. Similarly, the moment/rotation curve obtained from the 8-node mesh exceeds the limit load by 9 percent at this point in the deformation, but this curve is also quite flat.

At each point in the loading, the applied J was obtained from the moment/rotation curve in the following manner (see fig. 6). Following Rice et al. [7], we can equate J with the area between moment per unit thickness/rotation curves of specimens with slightly altered crack lengths by

$$J_{M\theta} = \int_0^M -(\partial\theta_{total}/\partial b)_M \, \mathrm{d}M, \tag{9}$$

where M is the moment per unit thickness, b is the remaining ligament, and θ_{total} is the total rotation of one end of the specimen relative to the other. The total rotation can be separated into the sum of the rotation which would occur in the absence of the crack, $\theta_{no\ crack}$ and an additional rotation due to the presence of the crack, θ_{crack}. Since $\theta_{no\ crack}$ represents the rotation of the uncracked beam, it is independent of the remaining ligament b, so that

$$\partial\theta_{total}/\partial b|_M = \partial\theta_{crack}/\partial b|_M . \tag{10}$$

Rice et al. [7] showed that, for deeply enough cracked specimens, θ_{crack} must have dependence on the moment M and the remaining ligament b only through the ratio M/b^2. However, finite element and collocation analyses have shown that the crack depth must be very deep indeed for the elastic part of the cracked rotation θ^e_{crack} to depend only on M/b^2. From the compilations of Tada et al. [24] the error which would be made in the computation of J in the linear moment rotation range by assuming θ^e_{crack} to depend only on M/b^2 would be roughly 6 percent for the considered crack depth-to-width ratio of 0.8. However, in unpublished work by the author the plastic portion of the rotation due to the presence of the crack, θ^p_{crack}, has been found to depend essentially on M/b^2 in even less deeply cracked specimens, at least in the fully plastic regime. Thus, θ_{crack} was separated into the sum of an elastic rotation (which is the product of moment and a known compliance function of relative crack depth) and a plastic rotation which depends on M/b^2. These forms are inserted into eqs. (9) and (10), and, following the standard steps, one obtains

$$J_{M\theta} = J_{elastic} + \frac{2}{b}\int_0^{\theta^p_{crack}} M\, \mathrm{d}\theta^p_{crack} = \alpha M^2/E'b^3 + (2/b)\int_0^{\theta^p_{crack}} M\, \mathrm{d}\theta^p_{crack}, \tag{11}$$

where the factor α is a pure number depending on relative crack depth, and E' is the appropriate elastic modulus, equal to the Young's modulus E for plane stress, and to $E/(1-\nu^2)$, where ν is Poisson's ratio, in plane strain.

The integral in eq. (11) was evaluated using the trapezoidal rule since load incrementation was accomplished in a series of linear steps.

The virtual crack extension method was applied at each load increment by separately advancing the inner ring of nodal points (and midside nodes in the 8-node elements) on each of the element rings surrounding the crack tip. The differencing procedure used to evaluate eq. (8) was found to be relatively insensitive to the size of the virtual crack extension, provided that the extension was of order 10^{-3} to 10^{-6} of a typical element dimension.

It should be noted that use of the node-moving procedure in conjunction with the modified variational principle of Nagtegaal et al. [22] requires a slight modification of the formulation presented in the preceding section. In particular, it is necessary to replace everywhere the hydrostatic part of W, $\kappa\epsilon_{kk}\epsilon_{mm}/2$ (where κ is the bulk modulus), by the corresponding term used in the variational procedure of Nagtegaal et al., namely $\kappa(\epsilon_{kk}\phi - \phi^2/2)$. In 4-node elements, ϕ is taken to be the volume average of the dilatation over the element [22]. The differences in computed J values using either expression for the hydrostatic strain energy is typically less than 1 percent on other than the crack tip ring of elements. However, in the crack tip elements the differences can be very large, and consistent results are obtained there only by using the same integrand as was used to obtain the original finite element solution.

The results of the 4-node element mesh problems will be discussed first. Each of the 6 rings of elements gave J values within a few percent of $J_{M\theta}$ at each load increment of both the hardening

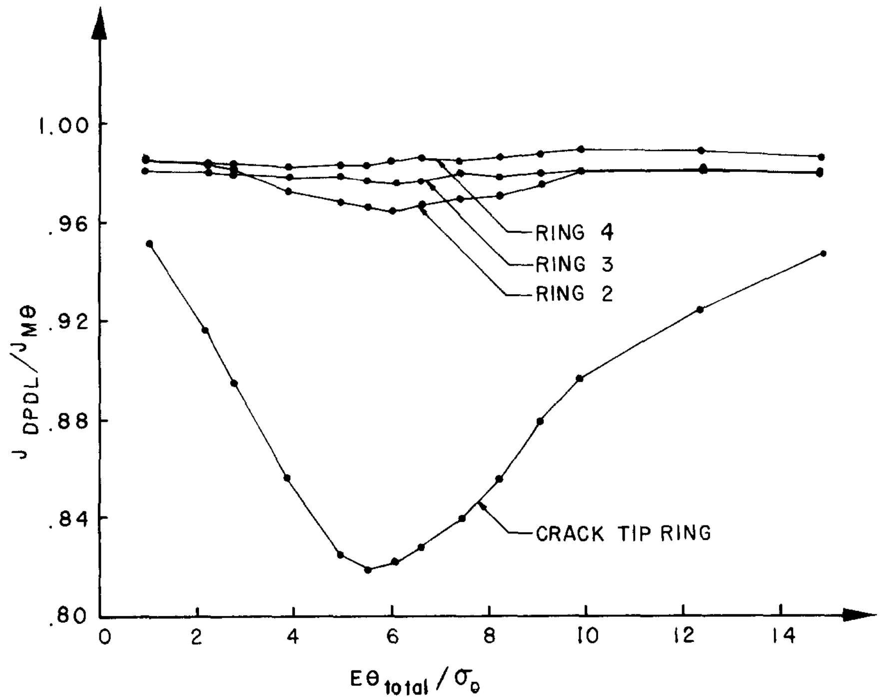

Fig. 7. J values obtained by virtual crack extension method on the 4 inner rings of elements in fig. 4 surrounding the crack tip as a function of overall deformation.

and the nonhardening solutions. Typical errors were of order 3 to 4 percent less than $J_{M\theta}$ in the hardening case, and 4 to 6 percent too low for the nonhardening case. The method was not particularly sensitive to the manner in which eq. (8) was numerically integrated. The best results for these elements were obtained using a 2 × 2 Gaussian scheme, although the results obtained using 2 × 1, 1 × 2 or even 1 × 1 Gaussian schemes were typically within 1 or 2 percent of the 2 × 2 results.

The error in the computed J values was generally greatest on the crack tip ring of elements. In the elastic load increment the computed J value was 7 percent below $J_{M\theta}$. This error decreases slowly to a roughly constant 5 percent below $J_{M\theta}$ in the nonhardening solution and 3 percent low in the hardening solution as fully plastic conditions are approached.

As an alternative to the nonunique crack tip displacement formulation in the problems just discussed, the mesh of 8-node quadrilaterals shown in fig. 4 was used. As was noted earlier, the displacements of all nodes located at the crack tip were constrained to be equal, so that no strain singularity results.

The results of the J computations for this mesh, normalized by $J_{M\theta}$, are shown in fig. 7. As can be seen, the J values inferred from the outer rings of elements are again in excellent agreement with $J_{M\theta}$ throughout the loading history. However, the values inferred from the crack tip ring of elements are not so accurate. At the elastic increment, the tip value is 5 percent low. Thus underestimate grows to a maximum error of roughly 18 percent below $J_{M\theta}$ at an overall deformation of $E\theta_{tot}/\sigma_0 \approx 5.5$. Subsequently, the error on this contour decreases as deformation continues and a fully plastic limit field is approached.

Unfortunately, these results do not provide a satisfactory determination of J from the crack tip contour alone. In fact, estimates obtained there tend to be nonconservative. The results in fig. 7 were for an incremental plasticity formulation, but quite similar results were obtained using deformation theory as well.

Poor results for the inner contour were also obtained in a perfectly plastic deformation theory solution of a plane strain center-notched panel. In this problem, 12 constant strain triangles were focussed to the crack tip. The inner contour J estimates were 11 percent low in the elastic increment, and the error increased steadily to a roughly constant 30 percent low in the fully plastic regime. Again, errors in the outer element rings were typically 2 to 5 percent low throughout the solution.

3. Summary

A new method of determining the ductile fracture parameter J from elastic-plastic finite element solutions has been presented. Numerical results in two-dimensional planar configurations show that good accuracy can be obtained from standard finite elements using fairly coarse discretizations. Similar results were obtained from incremental and deformation theory plasticity formulations.

The method is applicable to a broad class of displacement-based finite element formulations in both two and three dimensions, and no particular special crack tip formulation is required. Although the errors in evaluating J are generally greatest on the crack tip ring of elements, good accuracy was obtained on this contour using a nonunique crack tip displacement formulation with the modified variational principle of Nagtegaal et al. [22]. This offers the hope that good J estimates may be obtained from the crack tip elements alone in other formulations allowing nonunique crack tip displacements, such as the element recently suggested by Barsoum [25] or a three-dimensional generalization of it. The ability to obtain consistently accurate J estimates by advancing only crack front nodes would be most convenient, especially in three-dimensional applications.

Acknowledgement

This work was supported in part by the Energy Research and Development Administration under Grant E(11-1)-3084 to Brown University, and in part by the Yale Computer Center. I wish to thank Dr. D.K. Brown and, especially, Dr. H.D. Hibbitt of MARC Analysis Research Corporation for computational assistance. Finally, I am pleased to acknowledge many helpful discussions of this work with Professor J.R. Rice.

References

[1] D.M. Parks, A stiffness-derivative finite element technique for determination of elastic crack tip stress intensity factors, Int. J. Fract. 10 (1974) 487-502.

[2] J.R. Rice, A path-independent integral and the approximate analysis of strain concentration by notches and cracks, Trans. ASME, Ser. D, J. Appl. Mech. 35 (1968) 379–385.

[3] J.A. Begley and J.D. Landes, The J integral as a fracture criterion, in: Fracture toughness, ASTM STP 514 (ASTM, Philadelphia, PA 1972) 1-23.

[4] J.D. Landes and J.A. Begley, The effect of specimen geometry on J_{Ic}, in: Fracture toughness, ASTM STP 514 (ASTM, Philadelphia, PA, 1972) 24-39.
[5] K.B. Broberg, Crack-growth criteria and non-linear fracture mechanics, J. Mech. Phys. Solids 19 (1971) 407-418.
[6] G.A. Clarke, W.R. Andrews, P.C. Paris and D. Schmidt, Single specimen tests for J_{Ic} determination. Presented at the 8th National Symposium on Fracture Mechanics, Brown University, Providence, RI, (Aug. 1974).
[7] J.R. Rice, Mathematical analysis in the mechanics of fracture, in: H. Liebowitz (ed.), Fracture, Vol. 2 (Academic Press, 1968) 191–311.
[8] J.R. Rice, P.C. Paris and J.G. Merkle, Some further results of J-integral analysis and estimates, in: Progress in flaw growth and fracture toughness testing, ASTM STP 536 (ASTM, Philadelphia, PA, 1973) 231-245.
[9] D.J. Hayes, Some applications of elastic plastic analysis to fracture mechanics, Ph.D. Thesis, Imperial Coll. London, 1970.
[10] T.K. Hellen, On the method of virtual crack extensions, Int. J. Numer. Meths. Eng. 9 (1975) 187-207.
[11] H.D. Hibbitt, Private communication (1975).
[12] B. Budiansky, "A reassessment of deformation theories of plasticity, Trans. ASME, Ser. D, J. Appl. Mech. 26 (1959) 259–264.
[13] S.B. Batdorf and B. Budiansky, Polyaxial stress-strain relations of a strain-hardening metal, Trans. ASME, Ser. D, J. Appl. Mech. 21 (1954) 323-326.
[14] J.L. Sanders, Plastic stress-strain relations based on linear loading functions, Proceedings of 2nd U.S. National Congress of Applied Mechanics, ASME (1954) 445-460.
[15] R. Hill, The essential structure of constitutive laws for metal composites and polycrystals, J. Mech. Phys. Solids 15 (1967) 79-96.
[16] J.W. Hutchinson, Elastic-plastic behavior of polycrystalline metals and composites, Proc. Roy. Soc. Lond., Ser. A, 319 (1970) 247-272.
[17] S. Stören and J.R. Rice, Localized necking in thin sheets, J. Mech. Phys. Solids 23 (1975) 421-441.
[18] J.W. Hutchinson, Singular behavior at the end of a tensile crack in a hardening material, J. Mech. Phys. Solids 16 (1968) 13-31.
[19] J.R. Rice and G.F. Rosengren, Plane strain deformation near a crack tip in a power law hardening material, J. Mech. Phys. Solids 16 (1968) 1-12.
[20] J.R. Rice and D.M. Tracey, Computational fracture mechanics, in: S.J. Fenves et al. (eds.), Numerical and computer methods in structural mechanics (Academic Press, 1973) 585-623.
[21] D.M. Tracey, Finite element solutions for crack tip behavior in small scale yielding, Trans. ASME, J. Eng. Mat. Tech. 98 (1976) 146-151.
[22] J.C. Nagtegaal, D.M. Parks and J.R. Rice, On numerically accurate finite element solutions in the fully plastic range, Comp. Meths. Appl. Mech. Eng. 4 (1974) 153-177.
[23] A.P. Green and B.B. Hundy, Initial plastic yielding in notch bend tests, J. Mech. Phys. Solids 4 (1956) 128-144.
[24] H. Tada, P.C. Paris and G.R. Irwin, The stress analysis of cracks handbook (Del Research Corp., Hellertown, PA, 1973).
[25] R.S. Barsoum, Application of triangular quarter-point elements as crack tip elements of power law hardening material, Int. J. Fract. 12 (1976) 463-466.